

# Magnetic Field Angle Effects on Sheath Formation near a Flat Plate Surface with Applications to Hall Thrusters

*Presented at Joint Conference of 30th International Symposium on Space Technology and Science,  
34th International Electric Propulsion Conference and 6th Nano-satellite Symposium  
Hyogo-Kobe, Japan  
July 4–10, 2015*

Joseph Lukas\* and Michael Keidar†  
*The George Washington University, Washington, D.C., 20052, USA*

**Abstract:** A preliminary analysis of an inclined magnetic field, of varying strength, on sheath formation on an Aluminum oxide,  $Al_2O_3$ , flat plate is demonstrated. It was calculated, through previously developed particle-in-cell code, that at large magnetic field line angles, ions are repelled from the wall and a sheath collapse should occur. The experimental work done on  $Al_2O_3$  appears to match the findings of the code; that increasing the magnetic field angle results in a reduction in sheath thickness. The results from this experiment also match previous experimental work by showing that an increase in the magnetic field strength will increase the thickness of the sheath. These results suggest that a Hall Thruster chamber may be designed to reduce ion sputtering (channel erosion) and create a more controlled exit plume.

## Nomenclature

$A$	= Amperage
$A_p$	= Probe cross-sectional area
$E_{\perp}$	= Perpendicular electric field
$J$	= Current density
$n_e$	= Electron plasma density
$R$	= Solenoid radius
$\mu_0$	= Permeability
$N$	= Number of turns over electro-magnet
$I$	= Current
$m_{Ni}$	= Nickel ion mass
$q_e$	= Elementary charge
$\Omega$	= Electrical resistance
$T_e$	= Electron temperature in eV
$T$	= Tesla
$V$	= Voltage
$kg$	= kilogram
$Hz$	= Hertz
$m$	= meter

---

\*Ph.D. Candidate, Mechanical and Aerospace Engineering Department, Joseph.N.Lukas@gmail.com

†Professor, Mechanical and Aerospace Engineering Department, keidar@gwu.edu

## I. Introduction

A Hall Effect Thruster, or Hall Thruster, is a plasma propulsion device where the propellant is accelerated using an electric field. The main components of a Hall Thruster are: an inner anode, propellant feeding device, a chamber, an external magnetic field and a hollow cathode placed at the chamber exit to create an axial electric field. The cathode is heated to generate electrons, which migrate into the chamber as they are attracted to the inner anode. As the electrons enter the chamber, they become trapped in the radial magnetic field and begin to gyrate around the field lines. Neutral propellant with high atomic weight and low ionization potential, such as Xenon or Argon, enters the chamber near the anode. As the neutral atoms travel down the chamber, they begin to collide with the trapped electrons and start to ionize, typically with a +1 charge. Due to the potential difference in the electric field, the ions are then accelerated out of the chamber producing thrust. As the ions exit, they are able to pull out electrons resulting in a zero net charge plasma plume, thus avoiding possible contamination issues.

Whereas Hall Thrusters are an established propulsion system capable of producing milli-Newton levels of thrust with specific impulses in the 1500 to 3000 second range, two common issues still faced are: chamber wall erosion undergone from ion sputtering and high exit plume angles; both of these issues may be mitigated through the study of magnetic field inclination angles. The radial magnetic field lines responsible for trapping electrons and ionizing neutral particles become modified at the chamber walls and begin accelerating ions into those same walls, both eroding material, thus limiting the thruster lifetime, and deviating ions away from the exit resulting in a lower thrust efficiency<sup>1</sup>. This occurs because of the formation of a plasma sheath. A plasma sheath is a thin layer of, usually positive, charge that develops on the surface of materials immersed in plasma. As an object is placed into the plasma, the, usually, smaller, faster electrons will reach the object first creating a negative charge on the surface. As the potential keeps getting more negative, electrons will then begin to be repelled while ions will become attracted creating a thicker positive layer. The thickness of this layer is generally on the order of a few times the Debye Length, or the distance where electrostatic effects still exist in plasma, and is based on the plasma density and temperature. The sheath modifies the electric field structure at the wall and directs ions into it. By inducing highly inclined magnetic field lines, the plasma sheath will begin to collapse as an inclined electric field begins directing ions away from the wall. An optimized magnetic field line design can direct the ions into a narrow plume and optimize thrust levels.

## II. Effect of Oblique Magnetic Field on Sheath

The experimental design for this paper was based off of the simulation work in Ref. 1 and Ref 2. A simple axis-symmetric electrostatic particle-in-cell (ES-PIC) code was used to analyze a small region near the outer wall, where ions are treated as particles and electrons were represented as a fluid. It was found that increasing the magnetic field angle, measured from the wall normal, would lead to a reduced sheath thickness. The sheath reduction appears quite linear, as seen in Fig. 1, until an angle of 70° is reached where a sharp sheath collapse appears to occur.

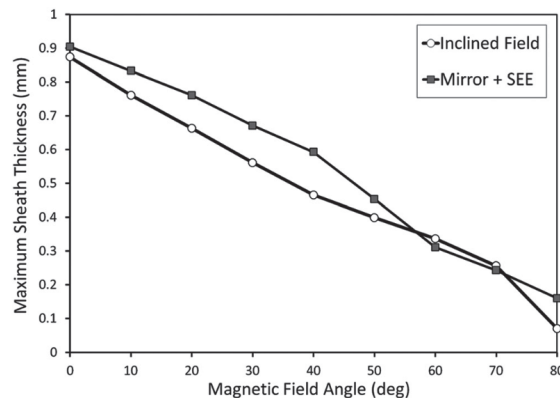


Figure 1. Sheath Thickness compared to Magnetic Field Angle<sup>1</sup>.

Figure 2 shows how increasing the magnetic field angle will change the shape of the sheath, seen in red, and begin to direct the ions away from the wall, as seen in the black streamlines. The presence of a  $40^\circ$  magnetic field inclination can result in a wall ion flux reduction of approximately 60 percent, which corresponds to a similar reduction in erosion rate. Another influence on sheath formation, from Ref. 1, includes the applied, perpendicular to the wall, electric field potential between the Hall Thruster anode and cathode. An electric potential,  $E_\perp$ , of  $20 \text{ kV/m}$  was used, and reducing this lead to a thicker sheath, while increasing to  $50 \text{ kV/m}$  lead to a full sheath collapse. The model also predicts that a sheath will form under an inclined magnetic field that has a small axial electric field.

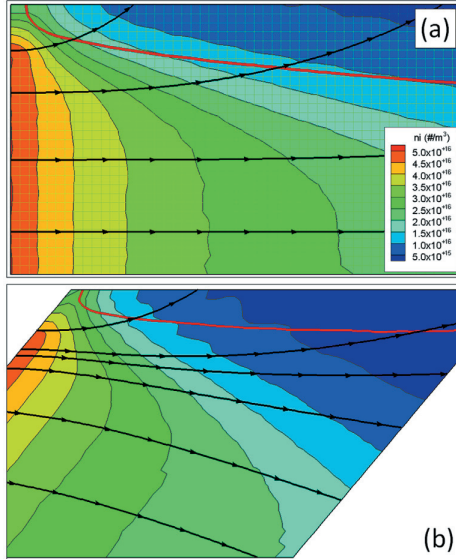


Figure 2. Sheath edge, in red, and ion trajectory, in black, for magnetic field line angles a)  $0^\circ$  b)  $40^\circ$ .

### III. Experimental Setup

A similar experimental setup to Ref. 3 was utilized, where an object is placed in-between two electro-magnetic solenoids and the sheath thickness can be measured using positively biased probes at various distances. The magnetic field from the solenoids can be used to control the thickness of the sheath, where a stronger magnetic field will produce a thicker sheath<sup>2</sup>.

#### A. Vacuum Chamber

Tests were carried out using a vacuum chamber, utilizing a roughing pump and a diffusion pump, capable of reaching a pressure of  $8 \times 10^{-5}$  Torr.

#### B. Helmholtz Coil

Two stainless steel electro-magnetic solenoids were used to create a magnetic field. To produce a homogeneous magnetic field in the mid-plane of the solenoids, a Helmholtz Coil was implemented. A Helmholtz Coil creates the homogeneous field through spacing the two identical solenoids at a distance equal to their radius and flowing a current in the same direction through the coils. The magnetic field along the centerline can be found using the following equation:

$$B\left(\frac{R}{2}\right) = \left(\frac{8}{5\sqrt{5}}\right) \frac{\mu_0 N I}{R} \quad (1)$$

With 520 turns (N), a solenoid radius (R) of 0.079883 meters, and a stainless steel permeability of  $1.26 \times 10^{-6} H/m$  ( $\mu_0$ ), the magnetic field lines have been plotted in MATLAB, Fig. 3, and using Finite Element Method Magnetics (FEMM)<sup>4</sup> simulation, Fig. 4, to show the uniformity, density and strength of the magnetic field lines.

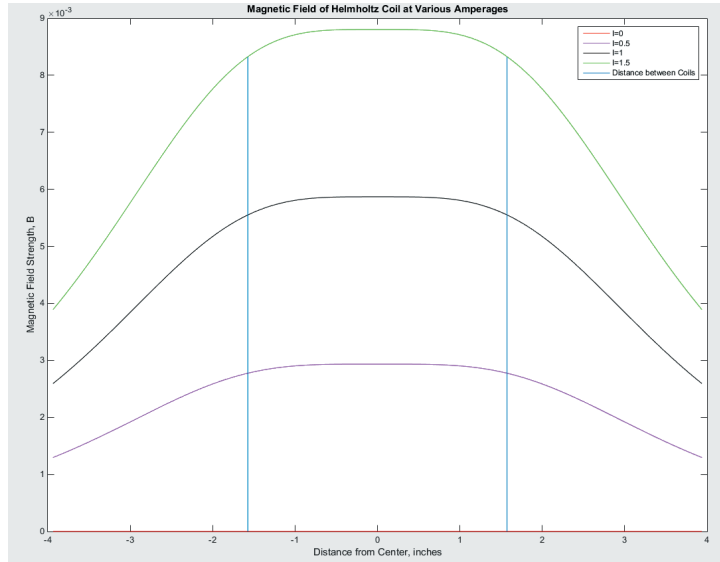


Figure 3. Magnetic field lines for a Helmholtz Coil at 0 Amps, 0.5 Amps, 1 Amp, and 1.5 Amps.

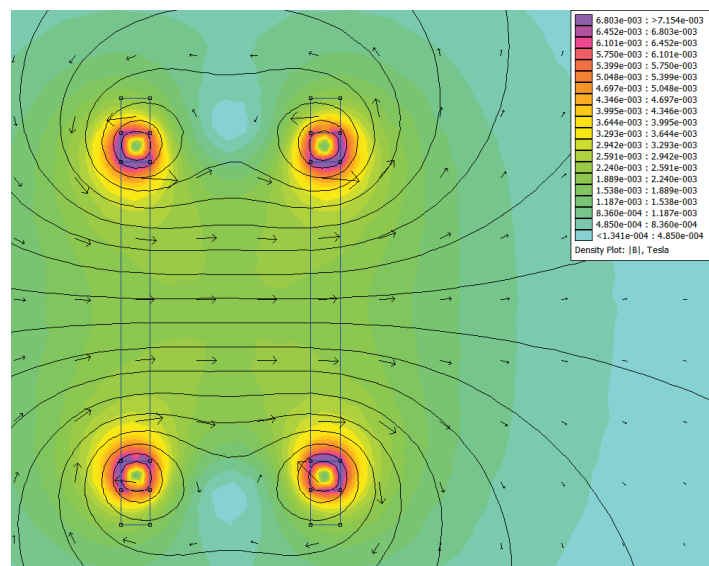


Figure 4. FEMM analysis for a planar view of a Helmholtz Coil at 0.5 Amps.

### C. $Al_2O_3$ Flat Plate

A 72 mm x 34 mm x 3.88 mm,  $Al_2O_3$  flat plate was attached to a rotating rod and placed through a vacuum pump flange to allow rotation inside the vacuum chamber from the outside. The rod and flange were designed to allow the flat plate to rest in the center of the Helmholtz Coil to experience a uniform magnetic field. A tubular spirit level was used on the flat plate to get an initial reading of  $90^\circ$  and a protractor was installed

on the outside of the chamber to allow full control on the plate's angle.

#### D. Electron Saturation Current Probes

Three copper, 4 mm x 2 mm x 0.17 mm probes were placed horizontally at the rear of the flat plate at heights of 1.5 mm, 6 mm and 10.5 mm from the its surface. These probes were biased to positive 74 V which would allow measurements of the electron current, and thus the sheath location. If the probe is immersed in the plasma, it will collect electrons, however, if the probe is immersed inside the sheath, the current reading will be close to zero as the sheath will be a positive charge layer void of electrons<sup>2</sup>.

#### E. Electric Field Probes

Two 12.25 mm x 7.83 mm x 0.5 mm copper probes were placed vertically, 22 mm apart from each other, vertically on one side of the flat plate. The front probe would be biased positively while the rear probe would be biased negatively. This would create an electric field, which will stay parallel to the rotating plate, that would simulate an acceleration zone inside a Hall Thruster. These probes were placed at different potentials (+1 V and -10 V, +1 V and -30 V, +1 V and -60 V, +10 V and -60 V, and +30 V and -60 V) to look at the electric field affect on sheath formation. A full image of the flat plate, electron saturation current probes and electric field probes can be seen in Fig. 5, and the flat plate between the solenoids can be seen in Fig. 6.

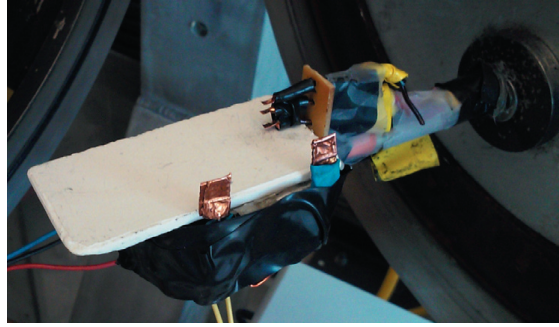


Figure 5. Flat  $Al_2O_3$  plate with two vertical electrical field probes and three horizontal electrical saturation current probes.

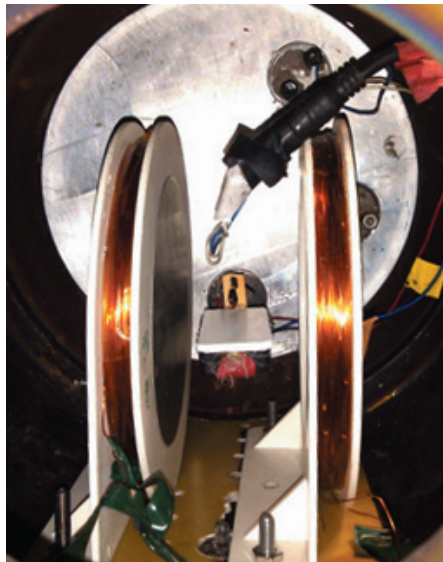


Figure 6. Flat plate between a Helmholtz Coil in the vacuum chamber.

## F. Plasma Source

A Micro-Cathode Arc Thruster ( $\mu$ CAT) was used as the plasma source for this experiment. A  $\mu$ CAT uses a vacuum arc between an anode and a cathode, over an insulator, to provide thrust by the ejection high velocity ions from an area called a cathode spot. The cathode spot occurs in a chaotic, retrograde fashion that emits electrons, ions, neutrals and macro-particles in the form of molten droplets. The vacuum arc is created using an inductive energy storage Power Processing Unit (PPU) which was set to produce a 50 Amp, 25 micro-second arc discharge at a pulse rate of 1 Hz. The propellant used was Nickel, which has an electron temperature of  $T_e = 1 - 2 \text{ eV}$  and ion mass of  $m_i = 9.7462 \times 10^{-26} \text{ kg}$ . The  $\mu$ CAT was placed a distance of 302 mm away from the front face of the electron saturation probes on the flat plate, and was angled away to reduce the plasma density and allow for a larger sheath to form.

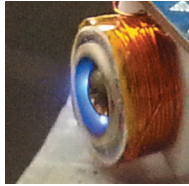


Figure 7. Pulsed  $\mu$ CAT thruster firing.

## IV. Data Collection

A Tektronix TDS 2004B oscilloscope was used to collect the electron voltage from the three probes (1.5 mm, 6 mm and 10 mm). The voltage was measured over 15  $k\Omega$  resistors to give the electron saturation current. Experiments were run such that five data graphs were collected over a combination of: every ten degree flat plate inclination, from zero to 90; applied magnetic fields of 0 Tesla, 0.0029 Tesla, 0.0059 Tesla, and 0.0088 Tesla; and applied electric fields (Front Probe/Rear Probe) of 0 V, +1 V/-10 V, +1 V/-30 V, +1 V/-60 V, +10 V/-60 V, and +30 V/-60 V, for a total of 1,200 trials. The five runs were then averaged together and the peak electron saturation current for each probe was recorded.

Knowing the electron saturation current, the electron plasma density can be found by using the equation for the current density,  $J$ :

$$J = \frac{I}{A_p} = n_e q_e \sqrt{\frac{T_e}{m_{Ni}}} \quad (2)$$

and re-arranging to solve for the electron plasma density:

$$n_e = \frac{I}{A_p q_e} \sqrt{\frac{m_{Ni}}{T_e}} \quad (3)$$

With a probe collection area,  $A_p$ , of  $3.4 \times 10^{-7} \text{ m}^2$ , assumed electron temperature of  $T_e = 2 \text{ eV}$ , particle charge of  $1.602 \times 10^{-19} \text{ C}$ , and an electron saturation current reading range between 0.000048 Amps to 0.001256 Amps, the electron plasma density is estimated to be between (variation being due to the various electric and magnetic fields used):

$$n_e = 4.86 \times 10^{17} \text{ m}^{-3} \text{ to } 1.27 \times 10^{19} \text{ m}^{-3} \quad (4)$$

## V. Results

Three parameters were evaluated to see their affect on the plasma sheath thickness: magnetic field angle, magnetic field strength, and electric field strength.

### A. Magnetic Field Angle

The experimental results of the magnetic field angle, which is the complementary angle to the flat plate angle, seem to match the theoretical predictions. Figure 8 and Fig. 9 show a decreasing sheath thickness with increasing magnetic field angle (an increasing electron saturation current indicates a lack of sheath). If a larger amount of trials are run, it is predicted these lines will move closer to linear. It is interesting to note that around  $70^\circ$  to  $75^\circ$ , there seems to be a sharp decrease in the sheath thickness, again, as predicted from the simulation.

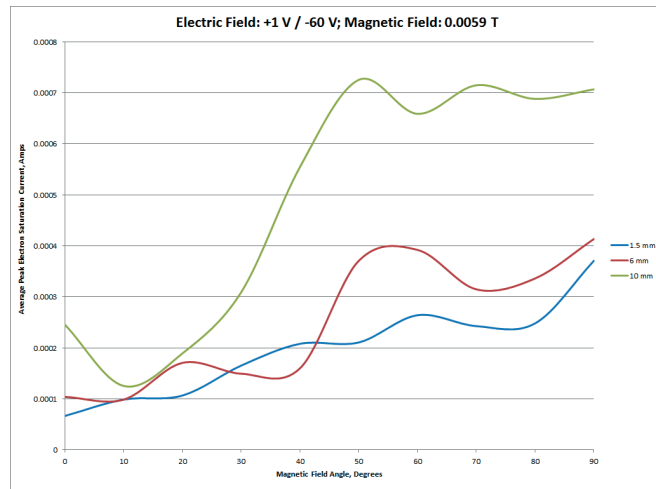


Figure 8. Electron saturation current for magnetic field line angles for an electric field of +1 V/-60 V at a magnetic field of 0.0059 Tesla.

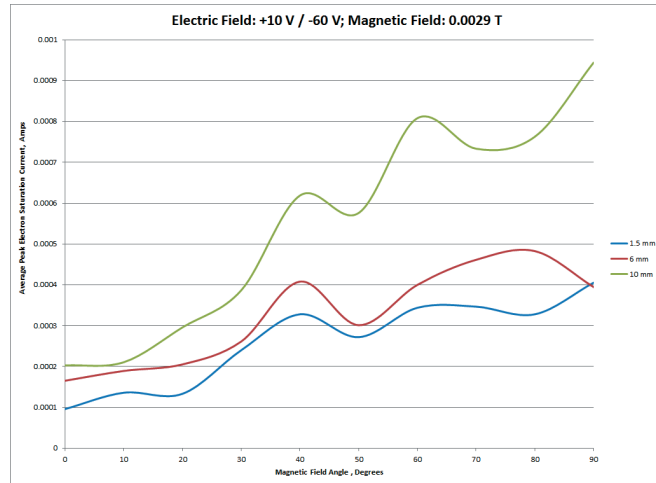


Figure 9. Electron saturation current for magnetic field line angles for an electric field of +10 V/-60 V at a magnetic field of 0.0059 Tesla.

## B. Magnetic Field Strength

The experimental results of the magnetic field strength also matched what was predicted; that an increase in magnetic field strength would increase the sheath thickness, as seen in Fig. 10.

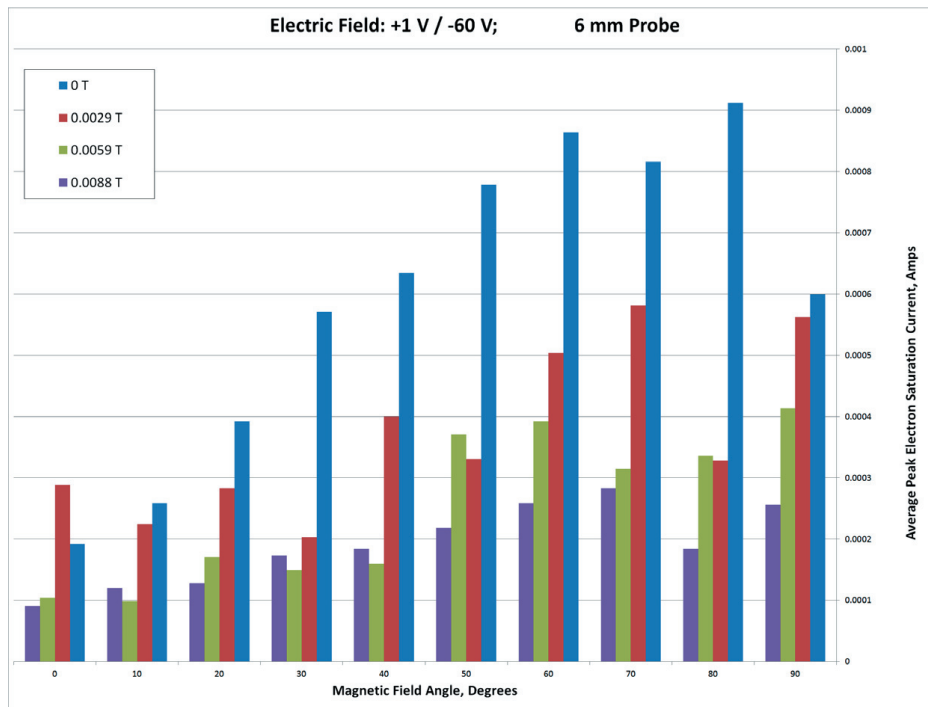


Figure 10. Peak electron saturation current for various magnetic field strengths for an electric field of +1 V/-60 V at the 6 mm probe.

## C. Electric Field

At this point in the analysis, the electric field strength is proving to be inconclusive. Below, Fig. 11, Fig. 12, and Fig. 13 show the peak electron saturation current, at the 6 mm probe, for 20°, 70°, and 90°, respectively.

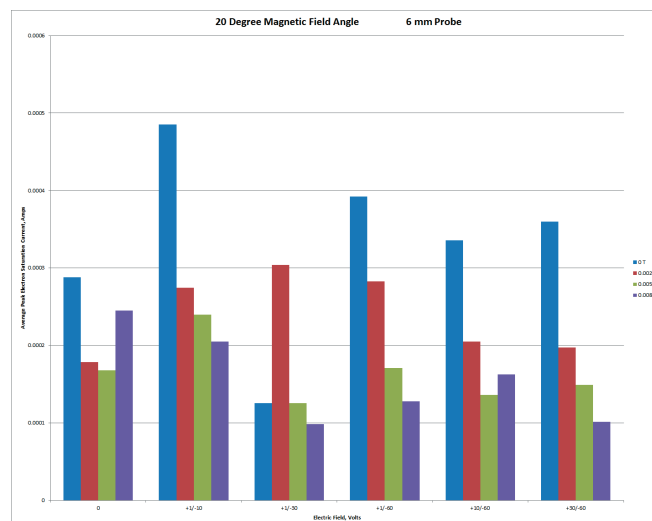


Figure 11. Peak electron saturation current for various electric fields at a 20° magnetic field angle at the 6 mm probe.



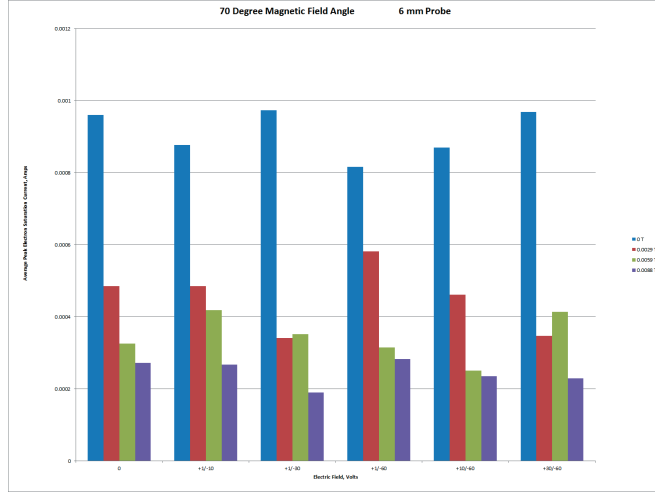


Figure 12. Peak electron saturation current for various electric fields at a 70° magnetic field angle at the 6 mm probe.

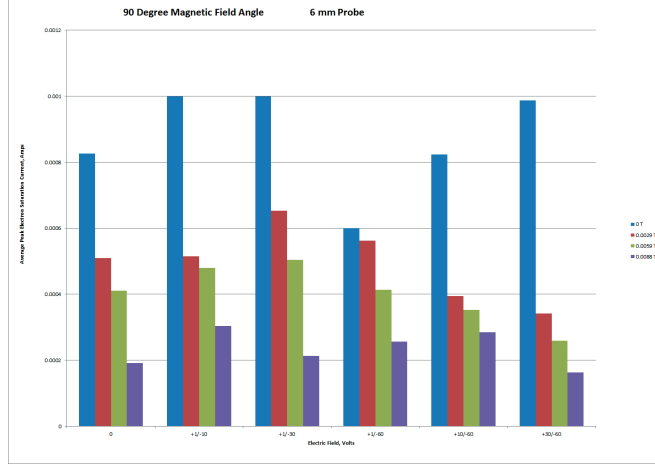


Figure 13. Peak electron saturation current for various electric fields at a 90° magnetic field angle at the 6 mm probe.

It is hypothesized that the electric field potential is not large enough compared to the simulation. The example used in Ref. 1 was a 200 V potential drop across a 1 cm wide acceleration zone.

$$E_{\perp} = \frac{\text{Potential Drop}}{\text{Acceleration Region Length}} = \frac{200 \text{ V}}{0.01 \text{ cm}} = 20 \frac{\text{kV}}{\text{m}} \quad (5)$$

With the experiment acceleration region over 22 mm, and the electric potential range going from 11 V to 90 V, the  $E_{\perp}$  range becomes 500 V/m to 4 kV/m which are well below the 50 kV/m needed to show a full sheath collapse.

## VI. Conclusion and Future Work

As this is only the preliminary analysis, a more in-depth review needs to be done to verify the results. However, both the magnetic field angle and magnetic field strength matched the predicted reactions for sheath thickness. The electric field strength is currently showing to be inconclusive, but it is surmised that

a larger electric potential is required. More trials should be run to see if the magnetic field angle and sheath thickness become more linear. The same trials for Boron-Nitride (BN) were also run, but the data still needs to be analyzed. BN has a higher sputtering coefficient than  $Al_2O_3$ , but a lower Secondary Electron Emission (SEE) yield, so it would be interesting to compare the two materials to see which responds better to the magnetic field angles. Having completed this, an internal chamber for a Hall Thruster can, hopefully, be designed and optimized to reduce chamber wall erosion and increase thrust efficiency.

## References

<sup>1</sup>Brieda, L., and Keidar, M., "Plasma-wall interaction in Hall thrusters with magnetic lens configuration," *Journal of Applied Physics*, Vol. 111, No. 12, 2012.

<sup>2</sup>Keidar, M., and Beilis, I. I., "Sheath and boundary conditions for plasma simulations of a Hall thruster discharge with magnetic lenses," *Applied Physics Letters*, Vol. 94, No. 19501, 2009.

<sup>3</sup>Keidar, M., Monteiro, O. R., Anders, A., and Boyd, I. D., "Magnetic field effect on the sheath thickness in plasma immersion ion implantation," *Applied physics letters*, Vol. 81, No. 7, 2002, pp. 1183-1185.

<sup>4</sup>FEMM, Finite Element Method Magnetics, Ver. 4.2, David Meeker, 2010.